ISSN No: 2348-4845
International Journal & Magazine of Engineering, Technology, Management and Research
A Peer Reviewed Open Access International Journal

AC-DC Unity Power-Factor Converter

Macharla Naveen
M.Tech(PEED),
Arjun College of Technology And Sciences.

Rosaiah Mudigondla, M.Tech (PEED),
Assistant Professor
Arjun College of Technology And Sciences.

ABSTRACT

This paper introduces a force converter and itscontrol circuit for high-recurrence sustained AC to DC change. In view of the resounding strategy, the info current is formed to be sinusoidal and is compelled to take after the high-recurrence sinusoidal information voltage in order to accomplish solidarity power element. With the best possible choice of the trademark impedance of the thunderous tank, the converter can play out the capacity of a buck, support or buck-help converter. The underlying state of the full tank is utilized to control the yield voltage increase of the converter. Since all the switches are worked at the essential recurrence of the info AC source, the exchanging loss of the converter is little. A control plan is additionally proposed for the converter. A proof-of-idea model working at 400 kHz is developed and its execution is tentatively measured. Comes about demonstrate that the proposed converter works as hypothetically foreseen.

Index Terms— ***AC to DC conversion, High frequency rectifier,Power factor correction, resonant technique, Wireless power transfer***

I. INTRODUCTION

Developing advances, for example, remote force exchange (WPT) regularly receive a high working recurrence in the extent from a couple of hundred of kHz to more than 10 MHz [1-4]. As of late, much research exertion has been committed to enhancing the execution of WPT frameworks as far as exchange separation and framework's vitality proficiency [5-9]. There is an absence of examination focusing on the ideal outline of the force converter at the collector side. Generally, the most straightforward methodology is to utilize a diode rectifier circuit with a yield stockpiling capacitor, as appeared in Figure 1(a) [10]. Be that as it may, this capacitor is charged to a worth near the pinnacle of the AC information voltage (see Figure 1(b)). Therefore, throbbing information current of huge greatness happens close to the pinnacle of the AC info voltage. Spasmodic current infers that remote force does not stream constantly from the essential side of the WPT framework to the yield of the framework. Such diode rectifiers draw exceptionally contorted current from the air conditioner power source and result in a poor info power variable (PF). The vitality proficiency and powertransfer ability of a poor PF framework are moderately low in view of the high conduction misfortune in the influence converters and transmission wires. Moreover, the bended current has a rich high-arrange symphonious substance which may bring about the outflow of electromagnetic impedance (EMI) that influences the operation of neighbor electronic hardware.

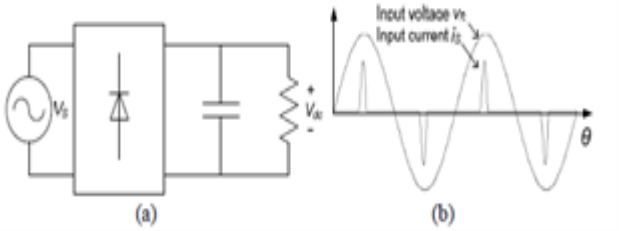

Figure 1. (a) A diode rectifier with a capacitor connected at the DC output side. (b) Input voltage and current waveforms.

ISSN No: 2348-4845
International Journal & Magazine of Engineering, Technology, Management and Research
A Peer Reviewed Open Access International Journal

A power electronic converter such as a boost converter can be used to shape the input AC current drawn by the rectifier to be sinusoidal and in phase with the AC voltage [11]. Figure 2(a) shows a classical boost converter connected after a diode bridge rectifier to form a power factor correction (PFC) circuit. The output DC voltage is sensed and fed to an error amplifier. The difference between the actual and reference voltage is derived and applied to a compensator circuit such as a proportional-integral (PI) compensator. The output of the compensator is multiplied with the signal proportional to the AC voltage waveform vS to produce the reference current signal iL,ref. Afterwards, a current- mode controller is used to generate the on and off signal to the switch shaping the current waveform of the inductor. Therefore, the average waveshape of the AC current is forced to follow the waveform of the AC voltage. Figure 2(b) depicts the input AC current waveform of the converter. It can be observed that the switching frequency of the PFC converter must be several times higher than the frequency of the AC system. Using a 400 kHz AC transmission system as an example, applying this current-shaping technology implies that the power switch has to operate in the tens of MHz. As a result, the switching loss becomes significant and the efficiency of the converter sharply reduces. Furthermore, MHz switching converter is also exposed to a number of problems arising from the passive and active components. For instance, the loss associated with the charging and discharging of the parasitic capacitance of power MOSFETs becomes significant [12-13].The high-frequency behavior of the devices is very different from that of the low-frequency behavior [14-15]. In terms of using passivecomponents in design, it is important to enhance their temperature stability and to minimize the unwanted stray and parasitic elements [15]. For the design of printed circuit board, it is crucial to eliminate undesired coupling between neighboring components and the rest of the circuit [16]. Without addressing these issues, the converter cannot be operated at a high frequency and achieved a high efficiency [17]. In [18-19], device-level packaging and circuit interconnection technologies are proposed to substantially reduce the structural parasitics and to improve the thermal management. However, the thermal performance and EMI are still big challenges which are difficult to solve individually as they are closely related to the circuit layout and packaging [20].

The paper is sorted out as takes after. In Section II, the idea of utilizing inductor-capacitor (LC) arrangement thunderous circuit to perform PF remedy will be presented. The working guideline of the proposed high-recurrence - encouraged air conditioning dc power converter will be unequivocally portrayed utilizing the comparing timing charts and identical circuit outlines. At that point, the voltage transformation proportion and proficiency of the converter will be scientifically researched and displayed in Section III. Subsequently, the development of a proof-of-idea model and its trial estimation results will be talked about. Area IV gives the finishes of the paper.

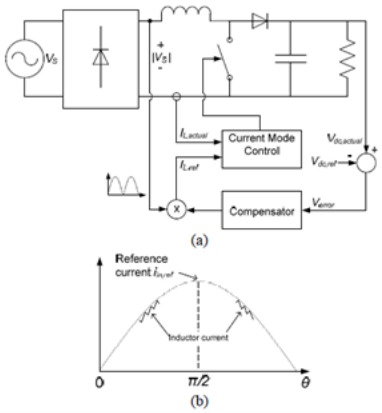

Figure 2. (a) A power factor correction circuit. (b) Input voltage and current waveforms.

II. TOPOLOGY AND OPERATING PRINCIPLE

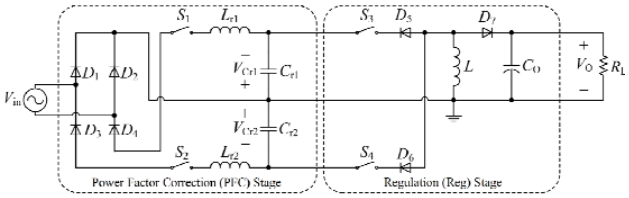

Figure 3.The proposed high-frequency-fed ac-dc power converter.

ISSN No: 2348-4845
International Journal & Magazine of Engineering, Technology, Management and Research
A Peer Reviewed Open Access International Journal

In this area, a high-recurrence bolstered air conditioning dc power converter is displayed as given in Figure 3 and its working and controlprinciples are clarified [21]. The profitable elements of this converter incorporate close solidarity information power variable and stand out exchanging activity per cycle for all the force switches.

A. LC Series Resonant Circuit

The force element molding property is performed utilizing the LC arrangement thunderous circuit at the info stage. The operation of the positive half cycle is utilized to portray how the LC full circuit can perform PF control in the high-recurrence air conditioning dc power converter. A rearranged circuit outline is appeared in Figure 4(a). Accept that the source recurrence is the same as the thunderous recurrence of the LC circuit ω=ωr=1/[2π(LrCr)1/2]and the underlying current of the resounding inductor is zero. There are two parameters that will influence the adequacy and waveform of the inductor current. The principal parameter is the equal impedance of the LC circuit which is planned by the thunderous inductor and capacitor with the end goal that ZLC=(Lr/Cr)1/2, and the second parameter is the underlying voltage of the resounding capacitor.

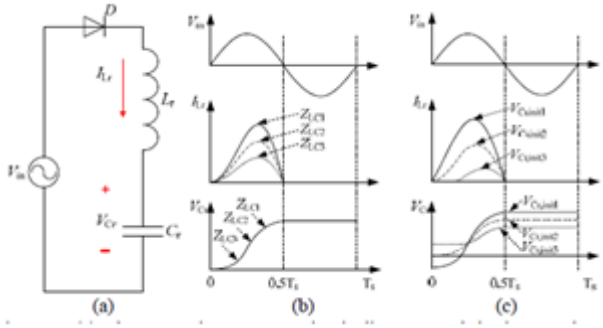

Figure 4. (a) The LC series resonant circuit diagram, and the input voltage, input current and resonant capacitor voltage waveforms: (b) with different equivalent impedance (Z_{LC}); Z_{LC1}<Z_{LC2}<Z_{LC3}, and (c) with different initial voltage of resonant capacitor $V_{Cr,init1}$< ($V_{Cr,init2}$=0) <$V_{Cr,init3}$.

Figure 4(b) demonstrates the current and voltage waveforms of the LC resounding circuit with various proportionate impedances in the positive half cycle of the information voltage. The underlying voltage of the thunderous capacitor and the current of the resounding inductor are zero (VCr,init = 0 and ILr,init = 0). It can be watched that the source current is influenced by the identical impedance of the LC circuit while the voltage waveform of the resounding capacitor continues as before. The aggregate vitality put away in the thunderous capacitor over the positive half cycle is relative to the span of the capacitance.

Figure 4(c) demonstrates the positive half cycle of the info voltage, the current of the full inductor, and the voltage of the thunderous capacitor of the same circuit however with various beginning conditions. It can be seen that the underlying voltage estimation of the thunderous capacitor can influence the extent of the full current of the inductor, of which the lower the underlying resounding capacitor voltage, the higher the full inductor current gets to be, and the lower the underlying resounding capacitor voltage, the higher the capacitor voltage gets to be toward the end of the half cycle.

B. Proposed Topology

The proposed two-phase circuit topology is appeared in FigureThe first stage (PFC stage) comprises of two switches, four diodes, two full inductors, and two thunderous capacitors. The second stage (control stage) comprises of two switches, three diodes, one inductor, and one capacitor. In the PFC arrange, the capacitor Cr1 and Cr2 are on the other hand charged by the information AC voltage source through the other exchanging activities of force switches S1 and S2. Cr1 is charged in the positive half cycle and Cr2 is charged in the negative half cycle.

In the direction arrange, the capacitors Cr1 and Cr2, which have been charged by the primary stage converter, is commutated on the other hand as vitality hotspots for the second-organize converter. Note that the second stage can be executed by a few sorts of force converters. In this paper, the buck-help converter was chosen for showing the proposed thought. The

ISSN No: 2348-4845
International Journal & Magazine of Engineering, Technology, Management and Research
A Peer Reviewed Open Access International Journal

proposed topology can accomplish high power element by utilizing the property of the arrangement thunderous circuit as examined in Section II-A.

C. Timing Diagram and Operating Modes

The planning graphs of the proposed high-recurrence bolstered air conditioning dc power converter are appeared in Figure 5(a). It can be seen that there are four working modes as appeared in Figure 5(b) to Figure 5(e). In the PFC stage, switches S1 and S2 are utilized to choose the resounding tanks Lr1-Cr1 and Lr2-Cr2 for the positive and negative half-cycles, separately. In the direction stage, S4and S3are the switches for controlling the buck-boostconverter for the positive and negative half-cycles, individually. Here, it is accepted that C = C and L = L .

Mode 1 (0 <t<t_1): Prior to turning the switchesS_1S_4on, the capacitor C_{r1} and C_{r2} are assumed to be charged to $V_{Cr,min}$and$V_{Cr,max}$, respectively. The positive half-cycle beginsat t=0. In the PFC stage, switch S_1 is turned on and switch S_2 is turned off. Diodes D_1 and D_4 are in the conducting state but diodes D_2 and D_3 are not conducting (see in Figure 5(b)). L_{r1} and C_{r1} are connected in series forming a series resonant circuit. The first half of the resonance takes place and the inductor current starts from an initial value (zero), follows the first half of a sinusoidal waveform and then decreases to zero as D_1 and D_4 block the reverse current flow. Meanwhile, the voltage of capacitor C_{r1} is charged from its initial value $V_{Cr,min}$ to a certain level at $t = t_1$.

In the control stage, switch S4 is turned on and diode D6 is in its directing state. Switch S3 is killed and diodes D5 and D7 are opposite one-sided. The inductor L is adequately extensive to such an extent that the present iL can be thought to be a steady greatness. Capacitor Cr2 and inductor L shape a shut circuit. Cr2is released in one bearing because of the extremity of diode D6until the voltage of capacitor Cr2is equivalent to the base voltage of capacitor Cr2(VCr,min) . The base voltage of capacitor Cr2 is either a positive voltage (VCr,min> 0), zero voltage (VCr,min = 0) or negative voltage (VCr,min< 0) contingent upon the yield power. Vitality is exchanged from the PFC stage to the direction arrange and is put away in the inductor L. In this day and age, the yield capacitor CO conveys vitality to the yield load resistor RL.

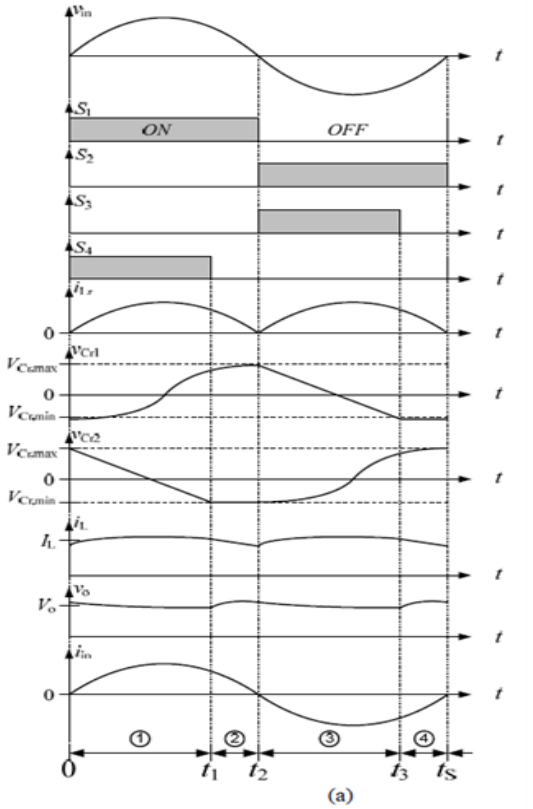

Figure 5. (a) Timing diagrams of the converter. Equivalent circuit diagrams in each operating mode: (b) Mode 1, (c) Mode 2, (d) Mode 3 and (e) Mode 4.

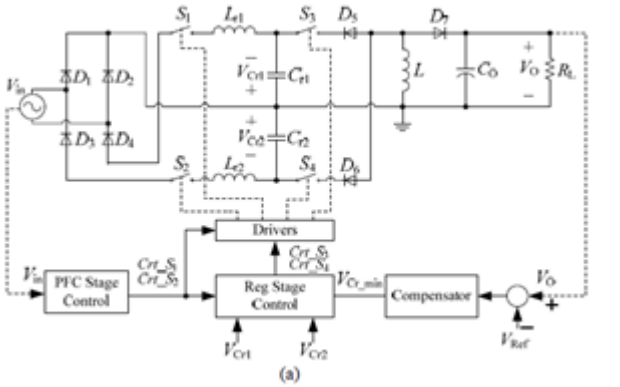

ISSN No: 2348-4845
International Journal & Magazine of Engineering, Technology, Management and Research
A Peer Reviewed Open Access International Journal

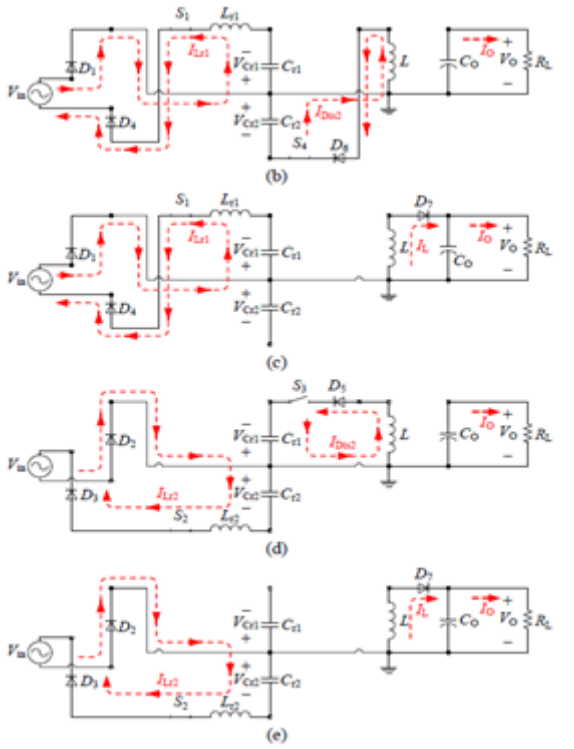

Figure 6. (a) Overall control block diagram, (b) control circuit of the PFC stage, and (c) control circuit of the regulation stage

Mode 2 (t_1<$t \leq t_2$): In the PFC stage, the functions of theswitches (S_1 and S_2) and diodes (D_1, D_2, D_3 and D_4) are the same as that in Mode 1. Thus, the capacitor C_{r1} is kept charging by the power source to the level $V_{Cr,max}$ at $t = t_2$, at which the positive cycle ends. Now, I_{Lr1} becomes zero and theswitch S_1 is commutated off naturally. The diodes D_1 and D_4 become non conducting. In the regulation stage, S_3 and D_5 remain in the off state. S_4 is turned off at $t = t_1$ and D_6 isreverse biased when the voltage of C_{r2} is equal to $V_{Cr,min}$. Now, capacitor C_{r2} is not connected to the PFC or the regulationstage. The current of inductor L cannot be changed instantaneously, resulting in the forward-biased conduction of diode D_7. Therefore, the energy stored in inductor L is delivered to the output capacitor C_O and the load resistor R_L.

Mode 3 (t_2<$t \leq t_3$): In the negative half-cycle ofv_{in}, the negative part of the waveforms are similar to that of the positive half-cycle. In the PFC stage, switch S_2 is turned on and switch S_1 is turned off. Diodes D_2 and D_3 are in the conducting state while diodes D_2 and D_3 are reverse biased (see in Figure 5(d)). Resonant tank L_{r2}-C_{r2} is connected in series with the input source V_{in}. The input current i_{in} is shaped as a sinusoidal waveform. The voltage on capacitor C_{r2} ischarged from the initial value $V_{Cr,min}$ to $V_{Cr,max}$. Energy is transferred from the input source V_{in} to capacitor C_{r2}. In theregulation stage, switch S_4 and diode D_6 remain in the off state. Switch S_3 is turned on. Diode D_5 is in the conducting state while D_7 is reverse biased. The energy stored in resonant capacitor C_{r1} is transferred to inductor L. C_{r1} is discharged to Luntil the voltage of capacitor C_{r1} is equal to $V_{Cr,min}$. Similarly to Mode 1, the load resistor R_L is supplied by the outputcapacitor C_O.

Mode 4 (t_3<$t \leq t_S$): In the PFC organize, the exchanging state ofthe switches (S1 and S2) and diodes (D1, D2, D3 and D4) are the same as that in Mode 3. In the direction stage, switch S3 isturned off at t = t3 when the voltage of Cr1 is equivalent to VCr,min. Vitality put away in inductor L is exchanged to yield capacitorCOand load resistor RLthrough diode D7. Its proportional circuitdiagram is appeared in Figure 5(e). Switch S2 is commutated off normally when info source Vin gets to be sure at t = tS. A short time later, switches S1 and S4 are turned on and the positive part of the operation is rehashed.

D. Control Methodology

Figure 6 demonstrates the control piece graph of the proposed high-recurrence bolstered air conditioning dc power converter. In the PFC arrange, the AC source voltage Vin is detected and sustained to a stage indicator circuit as appeared in Figure 6(b). The yields of the stage indicator circuit are associated with the driver circuit to control the on/off time of switches S1 and S2 taking after the AC source recurrence. The signs Crt_S1 and Crt_S2 are the control signs of switches S1 and S2, respectively.The yields of the stage locator are likewise connected to the beat width-regulation (PWM) generator to determine the control signals Crt_S3 and Crt_S4 for switches S3 and S4,

ISSN No: 2348-4845
International Journal & Magazine of Engineering, Technology, Management and Research
A Peer Reviewed Open Access International Journal

separately. The immediate yield voltage VO is detected and subtracted from the reference yield voltage VRef, of which the blunder is connected to a compensator to create the thresholdvoltage VCr,min for the full capacitors Cr1 and Cr2. Figure 6(c) demonstrates the control circuit of the direction stage where theinstantaneous voltage of the thunderous capacitors VCr1 and VCr2are being detected and contrasted with VCr,min with produce the heartbeat width of the switches S3 and S4. It is imperative to notethat the proposed control circuit can be acknowledged utilizing straightforward operational speakers and computerized rationale doors. Thus, they can be effectively created as a coordinated circuit (IC) for large scale manufacturing.

III. CIRCUIT ANALYSIS

A. Voltage Conversion Ratio

The derivation of the voltage conversion ratio of the proposed converter is presented in this section. For simplicity, all diodes and switches are considered ideal. In the PFC stage, an LC series resonant circuit is connected in series with the high-frequency AC source. The instantaneous current and voltage of the resonant inductor L_r and capacitor C_r in the half-cycle of the ac source can be described by equations (1) and(2). The detailed derivation of equations (1) and (2) are presented in Appendix A.

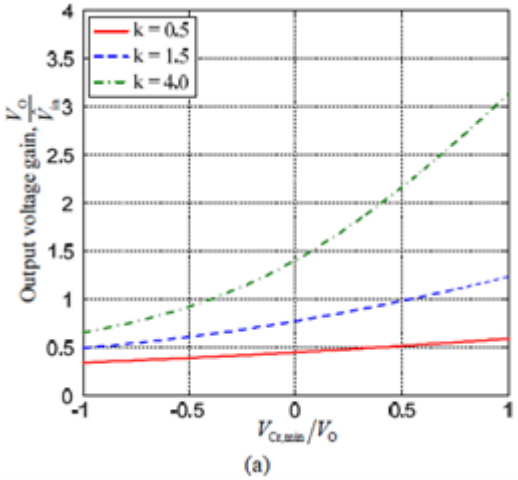

Figure 7. Plots of a) output voltage gain and b) output load variation versus normalized threshold voltage $V_{Cr,min}/V_{Cr.}$ where k= R_L/Z_{LC}

B. Efficiency of the Converter

The estimation of the individual efficiency of the PFC and the regulation stage is presented in this section on the assumption that the converter operates ideally with unitypower factor. From first principle, the energy consumption of the converter is found by integrating the instantaneous input power and it can be expressed as

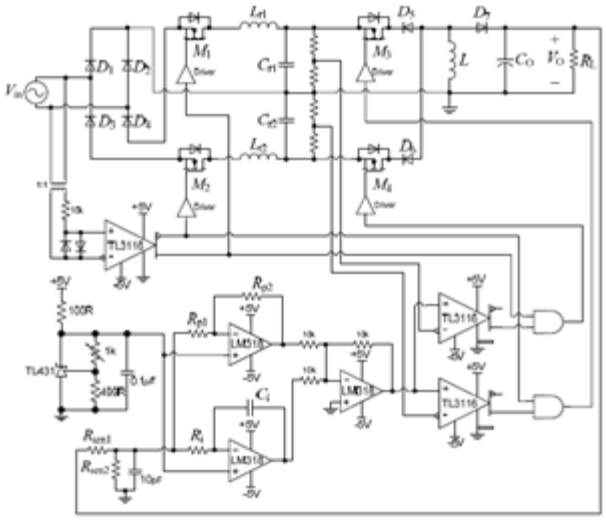

Figure 8.Schematic of the proposed high-frequency-fed ac-dc power converter.

IV. EXPERIMENTAL RESULTS

A. Voltage Conversion Ratio

A proof-of-concept prototype of the proposed high-frequency-fed ac-dc power converter is constructed. The control scheme is implemented using discrete components also, the circuit is appeared in Figure 8. The converter is intended to change over a 400 kHz AC voltage source into a DC source. The info voltage and the normal yield force of the converter are 50 Vrms and 30 W, individually. The yield load resistance of the converter is 100 Ω. Given the information AC voltage and the limit voltage VCr,min, the potential contrast over the resounding capacitor can be ascertained after condition (4). Disregarding the force loss of the circuit components, the information vitality over a large portion of an AC cycle is equivalent to the yield energydelivered to the heap over the same half cycle. The extent of the resounding capacitor can be resolved utilizing conditions (5) and

ISSN No: 2348-4845
International Journal & Magazine of Engineering, Technology, Management and Research
A Peer Reviewed Open Access International Journal

(6). As appeared in condition (7), the extent of the thunderous inductor is figured by prerequisite of the yield voltage of the converter. The exchanging gadgets utilized as a part of the model are CoolMOS transistors, which have a lower exchanging and conduction misfortunes than customary influence MOSFET in the high-recurrence range. Silicon-carbide Schottky (Sic) diodes are chosen in light of their low intersection capacitance, bringing about a low turn around recuperation current and force misfortune. The inductors and capacitors are business off-the-rack items. The itemized details of the segments are compressed in Table 1. Note that the determinations and test states of the converter are discretionary chosen to look at the operation of the converter. The trial of the converter is completed at three distinctive yield power levels at 11 W, 18 W and 30 W. The converter working waveforms are caught to check the hypothetical circuit examination. The related information current sounds and productivity of the converter are measured.

B. Experimental Results and Discussion

Figure 9 shows the captured waveforms of the input voltage, input current and resonant capacitors' voltages of the converter at different output power levels. The output power of the converter is increased from 11 W to 30 W when the threshold voltage is reduced from 25 V to −50 V. The converter is connected to a constant resistive load. Therefore, the output voltage changed from 29 V to 54 V accordingly. The experimental waveforms are in good agreement with the theoretical analysis given in Section II. In Figure 9 (a), it can be observed that the input current is distorted when the output power of the converter is low. In the other words, the delay angle α is not zero. The diodes in the PFC stage become reverse biased when the input voltage is lower than the initial voltage of the resonant capacitors. Nevertheless, a zero or negative initial voltage on the resonant capacitors causes the diodes to conduct at the beginning of each half cycle. As a result, the quality of the input current improves substantially as shown in Figure 9(b) and (c). Figure 10 shows the captured input current waveforms and their harmonic spectra using fast Fourier transform (FFT).

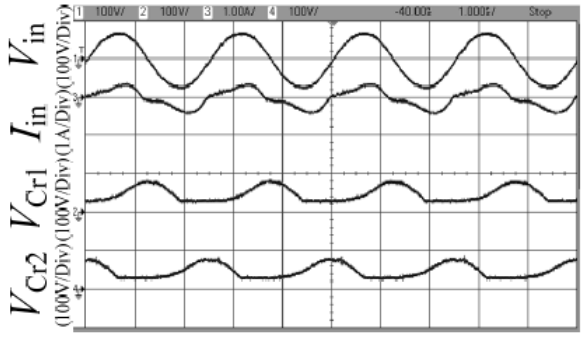

(a) $P_{out} = 11$ W

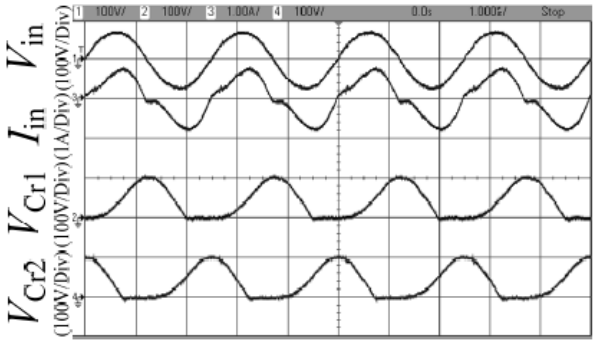

(b) $P_{out} = 18$ W

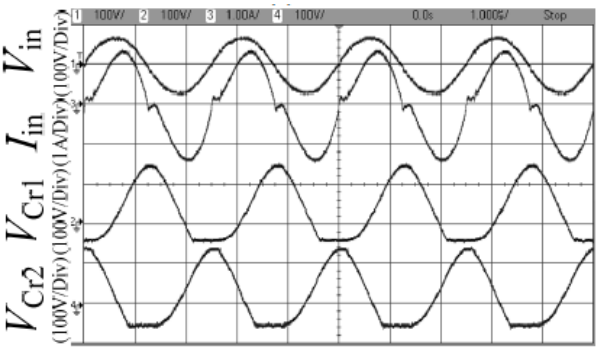

(c) $P_{out} = 30$ W

Figure 9:The waveforms of the input voltage, input current, and voltage of theresonant capacitors at different output power levels; (a) $V_{Cr,min}$ = 25 V, P_{out} = 11 W Cr,min = 0 V, *Pout* = 18 W and (c) *V*Cr,min = −50 V, *Pout* = 30 W.

The aggregate symphonious twisting (THD) of the info current at 11 W, 18 W and 30 W yield force are observed to be 22.66%, 19.88 and 14.38%, separately. Figure 11 demonstrates the caught yield voltage

ISSN No: 2348-4845
International Journal & Magazine of Engineering, Technology, Management and Research
A Peer Reviewed Open Access International Journal

waveform and its consonant range utilizing FFT. Since all the switches are worked in a synchronized way with the information AC source, the yield voltage contains a twofold line recurrence swell.

The AC info voltage and current are recorded by an advanced oscilloscope. Accordingly, the AC info force of the converter can be gotten by incorporating the result of the prompt information voltage and current. The DC yield force is measured by an advanced multi-meter. Consequently, the force component and general effectiveness of the converter are figured. Significant key execution records of the converter at various yield power levels are condensed in Table 2. It can be watched that the force variable of the converter at all the yield power levels can be kept up above 0.9. The productivity of the PFC and control stages are assessed utilizing conditions (9) to (14) as appeared in Table 2. They are all inside sensible extent from 80% to 90%.

The drop of effectiveness in the PFC stage is come about because of the high conduction loss of diodes and AC resistance of thunderous inductors. The productivity of the converter can be further enhanced by legitimate determination of parts as indicated by the fancied applications. The nitty gritty studies on the converter plan system, the inactive and active components' selection together with the optimization of the voltage conversion ratio and efficiency for practical high frequency AC-DC applications are left for further work.

Components	Symbols	Specifications
Resonant inductors	L_{r1} and L_{r2}	Coiltronics, UP3B-330-R 33uH, 3Ω@400kHz
Resonant capacitors	C_{r1} and C_{r2}	5nF 500V, ESR=0.15Ω@400kHz
Boost inductor	L	TDK-SLF12575T-221M1R3-PF, 220uH, 0.3Ω@DC,
Output Capacitor	C_O	220nF 630V, x 8
Transistors	M_1, M_2, M_3 and M_4	N-Ch CoolMos, IPD60R950C6, 650V, 4.4A, $R_{DS(ON)}$=0.95Ω
Diodes	D_1, D_2, D_3, D_4, D_5, D_6 and D_7	SiC Diode, C3D04060A, 600V, 7A, V_F=1.5V

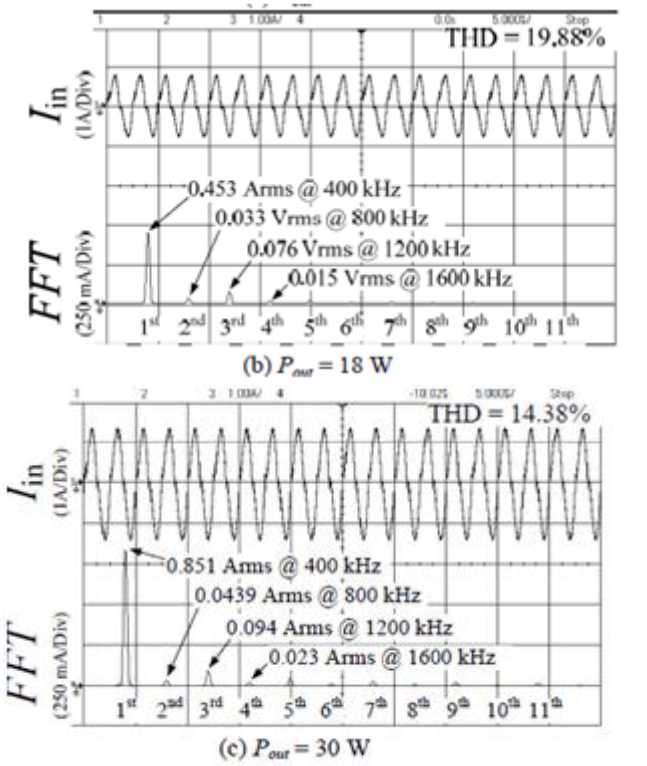

Figure 10. The waveform of the input current and its FFT at different outputpower levels; (a) *V*Cr,min = 25 V, *Pout* = 11 W (b) *V*Cr,min = 0 V, *Pout* = 18 W and (c) $V_{Cr,min}$ = −50 V, P_{out} = 30W.

TABLE 2.

Performance of the converter at different outputpower levels.

Parameters	Symbols	Conditions		
		I	II	III
Output power	P_O	11.63 W	17.99 W	30.39
Output	V_O	34.11 V	42.41 V	55.31
Output voltage	V_{rip}	0.56V	0.71 V	0.74 V
Input power	Pin	14.70 W	23.36 W	42.76
Input power	PF	0.95	0.94	0.93
Input current	Iin	0.308 A	0.496 A	0.918
Input current	THD-Iin	22.66 %	19.88 %	14.38
Threshold	$V_{Cr,min}$	25 V	0 V	−50V
Efficiency				
PFC stage	η_{PFC}	92.68 %	91.05 %	86.64%
Regulation	η_{Reg}	85.37 %	84.56 %	82.03%
Overall	η	79.13 %	76.99 %	71.08

ISSN No: 2348-4845
International Journal & Magazine of Engineering, Technology, Management and Research
A Peer Reviewed Open Access International Journal

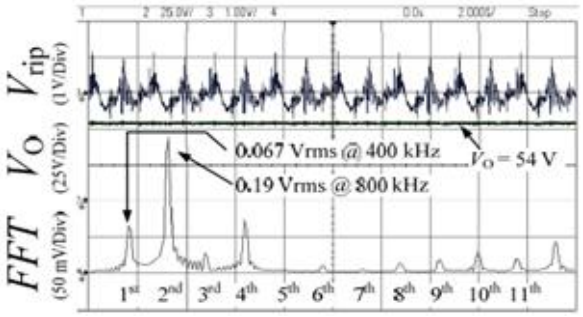

Figure 11. The waveforms of the output voltage, output voltage ripple and its FFT at $V_{Cr,min}$ = V, P_{out} = 30 W

V. CONCLUSION

A 400 kHz high-recurrence nourished AC-DC PFC converter with one exchanging activity for each cycle is illustrated. With a solitary converter topology, the converter can play out the capacity of a buck and support change contingent upon the trademark impedance of the resounding tank. The voltage transformation proportion of the converter can be further controlled by the underlying voltage of the thunderous capacitors. Exploratory results demonstrate that the converter can accomplish a powerful component (PF > 0.9) and a low information current twisting (THD < 20%). A control plan is likewise proposed for the converter. It can be acknowledged by basic operational enhancers and computerized rationale doors, and along these lines can be effortlessly created as an incorporated circuit (IC) for large scale manufacturing. The particular components of this converter are ideal for future high-recurrence AC power move framework working in the reach from a couple of hundred kHz to the MHz range.

REFERENCES

[1]N. Tesla, "Apparatus for transmitting electrical energy," U.S. Patent 1,119,732, Dec. 1, 1914.

[2]J. Schuder, H. Stephenson, and J. Townsend, "High-level electromagnetic energy transfer through a closed chest wall," Inst. Radio Engrs. Int. Conv. Record, vol. 9, pp. 119-126, 1961.

[3]J.C. Schuder, J.H. Gold and H. E. Stephenson, "An Inductively Coupled RF System for the Transmission of 1kW of Power Through the Skin", IEEE Transactions on Bio-Medical Engineering, Vol. BME-18, Issue 4, Page(s): 265 - 273, 1971.

[4]W. Ko, S. Liang, and C. F. Fung, "Design of radio-frequency powered coils for implant instruments," Medical and Biological Engineering and Computing, Vol. 15, Page(s): 634-640, 1977.

[5]M. Kiani, and M..Ghovanloo, "The circuit theory behind coupled-mode magnetic resonance-based wireless power transmission," IEEE Transaction on Circuits and Systems – I, Vol. 59, Issue 8, Page(s): 1-10, 2012.

[6]S. Cheon, Y.H. Kim, S.Y. Kang, M. L. Lee, J.M. Lee, and T. Zyung, "Circuit-model-based analysis of a wireless energy-transfer system via coupled magnetic resonances", IEEE Transaction on Industrial Electronics, Vol. 58, Issue 7, Page(s): 2906-2914, 2011.

[7]Y.H. Kim, S.Y. Kang, S. Cheon, M.L. Lee, J.M Lee and T. Zyung, "Optimization of wireless power transmission through resonant coupling", in Proc. CPE'09, Page(s): 426 - 431, 2009

[8]N.Y. Kim, K.Y. Kim, J. Choi and C.W. Kim, "Adaptive frequency with power-level tracking system for efficient magentic resonance wireless power transfer", Electronics Letters, Vol.48, No.8, 12 April 2012

[9]S.Y.R. Hui, D. Lin, C.K. Lee and J. Yin, " Methods for Parameters Identification, Load Monitoring and Output Power Control for Wireless Power Transfer", US patent application, July 2013.

[10]N. Mohan, T.M. Undeland and W.P. Robbins, "Power Electronics: Converters, Applications, and Design", 3 rd Edition, Page(s) 483 - 494.

ISSN No: 2348-4845
International Journal & Magazine of Engineering, Technology, Management and Research
A Peer Reviewed Open Access International Journal

[11]C. K. Tse, "Circuit Theory and Design of Power Factor Correction Power Supplies", IEEE Distinguished Lecture 2005, Circuit and Systems, http://cktse.eie.polyu.edu.hk/Tse-IEEElecture2.pdf.

[12]K. Gauen,"The Effect of MOSFET Output Capacitance in High Frequency Applications", in Proc. Industry Applications Society Annual Meeting 1989, Vol. 2, Page(s): 1227 - 1234, 1989

[13]M. Hartmann, H. Ertl and J.W. Kolar, "On the Tradeoff Between Input Current Quality and Efficiency of High Switching Frequency PWM Rectifiers", IEEE Transactions on Power Electronics, Vol. 27, Issue 7, Page(s): 3137 - 3140, 2012.

[14]Z. Chen, D. Boroyevich and J. Li,"Behavioral Comparison of Si and SiC Power MOSFETs for High-Frequency Applications", in Proc. Applied Power Electronics Conference and Exposition (APEC) 2013, Page(s): 2453 - 2460, 2013.

[15]Q. Li, M. Lim, J. Sun, A. Ball, Y. Ying, F.C. Lee and K.D.T. Ngo, "Technology Roadmap for High Frequency Integrated DC-DC Converter", in Proc. Power Electronics and Motion Control Conference 2009, Page(s): 1-8, 2009.

[16]W. Liang, J. Glaser and J. Rivas,"13.56 MHz High Density DC-DC Converter with PCB Inductors" in Proc. Applied Power Electronics Conference and Exposition (APEC) 2013, Page(s): 633-640, 2013.